Engineering Donor-Acceptor Conjugated Polymers for High-Performance and Fast-Response Organic Electrochemical Transistors

Hanyu Jia[1,‡], Zhen Huang[2,‡], Peiyun Li[1,‡], Song Zhang[3], Yunfei Wang[3], Jie-Yu Wang[2], Xiaodan Gu[3], and Ting Lei[1,4,*]

[1]Key Laboratory of Polymer Chemistry and Physics of Ministry of Education, Department of Materials Science and Engineering, College of Engineering, Peking University, Beijing 100871, China.

[2]College of Chemistry and Molecular Engineering, Peking University, Beijing 100871, China.

[3]School of Polymer Science and Engineering, The University of Southern Mississippi, Hattiesburg, MS 39406, USA.

[4]Beijing Key Laboratory for Magnetoelectric Materials and Devices, Peking University, Beijing 100871, China.

[‡]These authors contributed equally to this work.

*Correspondence and requests for materials should be addressed to T.L. (tinglei@pku.edu.cn).

Abstract: To date, high-performance organic electrochemical transistors (OECTs) are all based on polythiophene systems. Donor-acceptor (D-A) conjugated polymers are expected to be promising materials for OECTs owing to their high mobility and comparatively low crystallinity (good for ion diffusion). However, the OECT performance of D-A polymers lags far behind that of the polythiophenes. Here we synergistically engineered the backbone, side chain of a series of diketopyrrolopyrrole (DPP)-based D-A polymers and found that redox potential, molecular weight, solution processability, and film microstructures are essential to their performance. Among the polymers, P(bgDPP-MeOT2) exhibited a figure-of-merit (μC*) of 225 F cm^{-1} V^{-1} s^{-1}, over one order of magnitude higher than previously reported D-A polymers. Besides, the DPP polymers exhibited high hole mobility over 2 cm^2 V^{-1} s^{-1}, significantly higher than all D-A polymers employed in OECTs, leading to fast response OECTs with a record low turn-off response time of 30 μs. The polymer also exhibited better stability than polythiophene systems with current retention of 98.8% over 700 electrochemical switching cycles. This work provides a systematic solution to unleash the high-performance and fast-response nature of D-A polymers in OECTs.

Keywords: conjugated polymers, organic electrochemical transistors, diketopyrrolopyrrole polymers, operation stability, fast response

Introduction

Organic mixed ionic and electronic conductors (OMIECs), especially polymers, have attracted increasing attention because they can be low-temperature processed, facilely chemically modified, and readily electrochemically doped, while having good ion transport channels and “soft” biological interface.[1] OMIECs have been used for a wide range of applications including sensors, optoelectronics, bioelectronics, and energy

storage devices.[2] Among these devices, organic electrochemical transistors (OECTs) are particularly attractive because they couple both ionic and electronic inputs to modulate the channel conductance of a transistor in aqueous environment. OECTs have demonstrated their utility in transducing and amplifying low amplitude electrophysiological signals,[3-5] metabolite sensors,[6-8] and neuromorphic computing.[9,10]

To evaluate the performance of an OECT material, the following equation is often used (Equation 1):

$$g_{\mathrm{m}} = \frac{W}{L} \cdot d \cdot \mu \cdot C^{*} \cdot (V_{\mathrm{Th}} - V_{\mathrm{GS}}) \quad (1)$$

where g_{m} is the transconductance in the saturation regime; I_{DS} is the drain current; L, W, d are the channel length, width, and film thickness, respectively; μ is the charge carrier mobility; C^{*} is the volumetric capacitance, V_{Th} is the threshold voltage, and V_{GS} is the applied gate voltage. Recently, the product of μ and C^{*} has been proposed to benchmark an OECT material and to realize a better comparison between different materials. μC^{*} is the intrinsic property of a material independent of device geometry and bias condition. The higher the μC^{*} of the channel material, the more excellent the performance of an OECT under certain device geometry and operating conditions.

Response speed is another important factor of an OECT device, which is particularly important for applications, such as real-time neural signal amplification, high-quality bio-interfacing transmission, and neuromorphic simulation.[4,11,12] Notably, the response speed of OECTs is usually slower than that of organic field-effect transistors (OFETs) because both polymer swelling and ion diffusion are involved. The slow speed substantially limits the applications of OECTs in applications requiring fast signal response.[13] A recent study reveals that when employing an extremely short gate-to-channel length, the response speed of an OECT is limited by hole/electron mobility rather than ion diffusion/redistribution.[14] Therefore, conjugated polymers with high charge carrier mobility are desired for OECTs.

Recently, several thiophene-based conjugated polymers functionalized with ethylene glycol (EG) side chains, e.g. P(g2T-TT),[15] P(g2T-T),[16] and P(g2T2-g4T2)[17] have been developed. These polythiophene systems have exhibited high μC^{*} over 100 F cm^{-1} V^{-1} s^{-1}, outperforming the conventional materials poly(3,4-ethylenedioxythiophene):poly(styrenesulfonate) (PEDOT:PSS)[18] and its derivatives, e.g. Crys-P,[19] in many aspects. However, it is also should be noted that the backbone and the corresponding energy level of polythiophene systems are facing the problem of limited tunability, leaving no room for the development of n-type conjugated polymers, which hampers the application of OECTs in CMOS-like logic circuit and bioelectronics.[20,21]

Donor-acceptor (D-A) conjugated polymers have made great advances in the past few years, and their device performances have ranked the top positions in many organic electronics fields, including OFETs,[22] organic photovoltaics (OPVs),[23] and organic thermoelectrics (OTEs).[24] The good backbone planarity, low energetic disorder, and strong interchain interactions make D-A polymers successfully realize high charge carrier mobility with low crystallinity or near amorphous films (Figure 1).[25] Very

recently, several D-A polymers, using isoindigo (IID), naphthalenediimide (NDI), and pyridine-flanked diketopyrrolopyrrole (PyDPP) building blocks, have been developed as the OECT channel materials.[26-29] These materials have shown huge potentials for OECTs, including (i) diverse structures that provide vast exploration space and possibilities (ii) large regulation range of frontier orbital energy level to achieve n-type polymers and prevent side-reactions during device operation.[29] Unfortunately, these D-A polymers onlyexhibited moderate OECT performance with inferior μC^* (<10 F cm^{-1} V^{-1} s^{-1}) and slow temporal response (>100 ms) which have not shown the full potential of D-A polymers from our perspective. The performance-limiting factors of D-A polymers are unknown and essential to alter the situation.

To explore the performance-limiting factors of D-A polymers, here, we report a series of diketopyrrolopyrrole (DPP)-based D-A polymers copolymerized with various donor moieties and grafted with linear or branched EG side chains. DPP was specially chosen because its copolymers have shown high charge carrier mobility in OFETs.[30] Through donor, side chain, polymerization method, and processing solvent engineering, we successfully realized high figure-of-merit OECTs with μC^* of up to 225 F cm^{-1} V^{-1} s^{-1}, high carrier mobility over 2 cm^2 V^{-1} s^{-1}, and fast temporal response. The μC^* values are over one order of magnitude higher than previously reported D-A copolymers.

Results and discussion

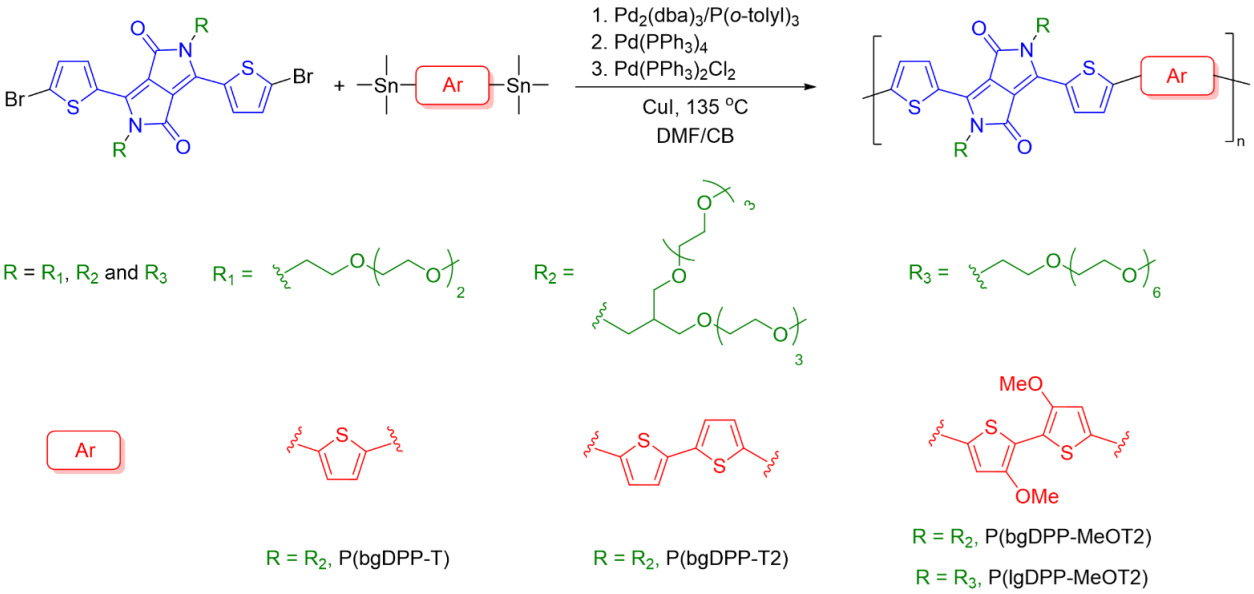

Scheme 1 Synthesis and chemical structures of DPP D-A polymers with different donor moieties and grafted with linear or branched ethylene glycol side chains.

Several donor moieties with increased electron-donating properties, e.g. thiophene, 2,2'-bithiophene, and 3,3'-methoxy-2,2'-bithiophene (Scheme 1), were used as the donor to tune the highest occupied molecular orbital (HOMO) energy level of the polymers. Similar to previous studies,[15,16] triethylene glycol (R_1 in Scheme 1) was

first used as the side chains. However, the strong π-π stacking interactions of DPP moiety made all the polymers insoluble after polymerization. Therefore, branched EG side chains (R_2 in Scheme 1) were employed to increase the solubility of the polymer. We found that when the monomer grafted with branched EG chains, Stille polymerization using $Pd_2(dba)_3$/P(*o*-tolyl)$_3$ as the catalyst only yielded oligomers and unreacted monomers. D-A polymers grafted with EG chains synthesized with similar polymerization conditions inliterature only showed low molecular weights (<10 kDa),[26] consistent with our results. After several trials, we found that $Pd(PPh_3)_4$ or $Pd(PPh_3)_2Cl_2$ can provide obviously higher molecular weight polymers when using *N*,*N*-dimethylformamide (DMF) as the solvent. We hypothesize that the branched EG side chains may inhibit the catalytic activity of $Pd_2(dba)_3$/P(*o*-tolyl)$_3$, probably due to the bulky P(*o*-tolyl)$_3$. Our observations are supported by previous studies using PEG as the side chains for Stille cross-coupling reactions.[31] To prevent the precipitation of polymers caused by the decreased polymer solubility in DMF, we used DMF/chlorobenzene 1:1 mixture as the solvent. CuI was added to accelerate the rate of transmetalation for higher molecular weight.[31] We observed that the reaction rate significantly increased as the reaction mixture turned into deep blue in a few minutes, and higher molecular weight polymers can be obtained.

Unlike D-A polymers with alkyl side chains, whose molecular weight can be evaluated using high-temperature GPC (HT GPC, usually 150 °C) and 1,2,4-tricholorobenzene (TCB) as the eluent,[24] these polymers did not show reasonable molecular weight or observable signals using HT GPC. This is probably due to the hydrophilic side chains since we observed that even though the polymers are visually dissolved in common aromatic or chlorinated solvents (e.g. *o*-DCB and chloroform), after spin-coating, the polymer films showed large chunks (Figure S1). After trying several eluents, we found that polar solvent hexafluoroisopropanol (HFIP) is a good eluent for molecular weight characterization. When using chloroform as the eluent, the polymers showed high molecular weights with M_n in the range of 61~71 kDa. In contrast, the molecular weights measured using HFIP showed M_n in the range of 26~30 kDa, suggesting the disaggregation of the polymers in HFIP (Table S1 in the Supporting Information (SI)). These molecular weight values are comparable to their alkyl side chain counterparts.[32] To understand the side-chain effects (linear *vs.* branched), a longer linear EG side chain (R_3 in Scheme 1) with the same number of EG segment ($-OCH_2CH_2-$) was used, yielding polymer P(lgDPP-MeOT2). The long linear glycol chains cannot provide enough solubility and only part of the polymers was Soxhlet extracted, giving a low yield of 26%. All the polymers exhibited good thermal stability with the decomposition temperature over 300 °C (Figure S2).

The optoelectronic properties of the polymers were evaluated using UV-Vis-NIR absorption spectroscopy and cyclic voltammetry (CV). The polymers exhibit a gradual red-shift of absorption maxima when replacing the donor moiety with a stronger electron-donating unit, no matter in solution, film, or annealed film (Figure 1a and Figure S3). DPP polymers containing the most electron-rich donor, namely MeOT2, including P(lgDPP-MeOT2), and P(bgDPP-MeOT2), exhibited smaller bandgap than P(bgDPP-T) and P(bgDPP-T2) (Table S2). Therefore, introducing a stronger electron-donating moiety (MeOT2) can remarkably lower the bandgap, largely due to increased HOMO energy levels and enhanced intrachain charge transfer. Interestingly, P(lgDPP-MeOT2)

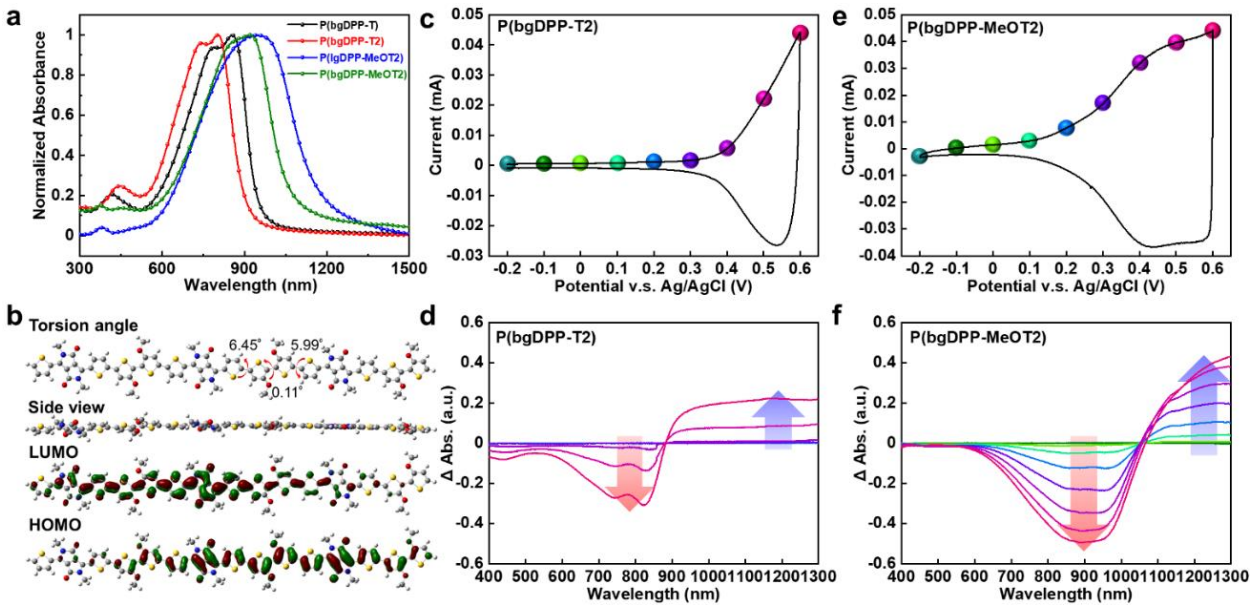

Figure 1 (a) UV-Vis-NIR spectra of spin-coated films of the four polymers after annealing. (b) DFT-optimized geometries and molecular frontier orbitals of the trimer of DPP-MeOT2. Calculations were performed at B3LYP/6-311G(d,p) level. Side chains were replaced with methyl groups to simplify the calculation. (c, e) Cyclic voltammograms and (d, f) differential electrochemical absorption spectra of DPP polymers with branched EG side chains. The color-coding UV-Vis-NIR spectra indicate the applied voltage, ranging from −0.2 V to 0.6 V with an interval of 0.1 V. The variation trends of spectra were highlighted with arrows.

with linear chains exhibited more redshifted absorption than P(bgDPP-MeOT2) with branched side chains. These results were further confirmed by CV measurements (Figure S5-S6 & Table S2). According to the ionization potentials (IPs) extracted from CV, DPP polymers with MeOT2 donor possess lower IPs of 4.62 eV for P(bgDPP-MeOT2) and 4.35 eV for P(lgDPP-MeOT2), suggesting that they are more susceptible to oxidation than P(bgDPP-T) and P(bgDPP-T2). DFT calculations showed that all the polymers exhibited planar backbones with small dihedral angles (Figure 1b and Figure S7). The HOMO was delocalized along the backbone, whereas the LUMO was largely localized on the DPP unit. Since linear side chains provide less interchain steric hindrance, we will prove later that P(lgDPP-MeOT2) has a closer molecular packing. This will lead to more planar backbones and increase the delocalization of the HOMO, thus leading to a higher HOMO level and smaller bandgap.

Spectroelectrochemistry was used to evaluate the electrochemical activity of the DPP polymers, by virtue of its consecutive and controllable electrochemical doping under programmable bias conditions. The changes in absorption spectra and current density upon different potential were monitored in 0.1 M NaCl aqueous solution. All polymers exhibited reversible and stable electrochemical redox features over 20 CV cycles (Figure S5). Gradually increasing the bias voltage from −0.2 to 0.6 V, three DPP polymers with different donors exhibited different electrochromic activities (Figures 1c-1f & Figures S7-S8). Concretely, both P(bgDPP-T) and P(bgDPP-T2) exhibited a partial extinction of π-π* absorption band (650-850 nm) and a gradually increased polaron

absorption band (1000-1300 nm). It is notably that the absorption variations of P(bgDPP-T) and P(bgDPP-T2) at 750 nm and 1100 nm are not obvious until applied bias exceeds 0.3 V, higher than that (0.1 V) of P(bgDPP-MeOT2). To quantify the oxidation degree of the films during the electrochemical scan, differential spectra of DPP polymers were calculated to highlight the absorption variation by subtracting the spectrum of each film recorded under their neutral states (Figure 2).[33] Clearly, P(bgDPP-MeOT2) exhibited a more significant absorption variation in the π-π* absorption band (750-1050 nm) and the polaron absorption band (1050-1300 nm). These results indicate that P(bgDPP-MeOT2) is more liable to be p-doped in the aqueousenvironment. Similar results were also found in the linear chain polymer P(lgDPP-MeOT2), which is even more facile to be oxidized due to its increased HOMO energy level (Figure S8).

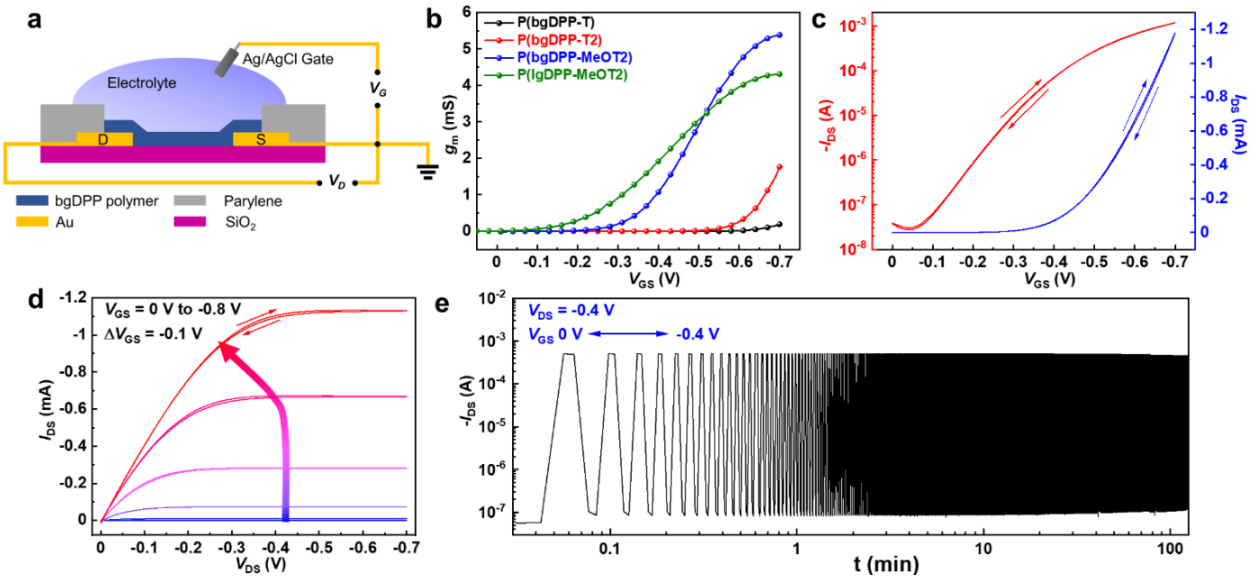

Figure 2 OECT device structure and the device characteristics of P(bgDPP-MeOT2). (a) Schematic illustration of the OECT device structure in cross-section view and wiring diagram for device operation. (b) Transconductance curves of P(bgDPP-T), P(bgDPP-T2), P(lgDPP-MeOT2) and P(bgDPP-MeOT2). (c) Transfer and (d) output characteristics of P(bgDPP-MeOT2) OECTs. V_{DS} = −0.6 V. (e) Long-term on-off switching of P(bgDPP-MeOT2) operated with the indicated V_{DS}, V_{GS} values. Switching on time of V_{GS} and the interval time were set as 2 s both. All OECTs were measured in 0.1 M NaCl aqueous solution. W/L = 1000/10 μm in all devices.

OECTs were fabricated using photolithography and parylene patterning method according to literature.[18,34] We explored many solvents for device fabrication, including *o*-DCB, chlorobenzene (CB), chloroform, trichloroethane, and HFIP. We found that except for HFIP, other solvents cannot provide good device performance (g_m usually < 0.1 mS for P(bgDPP-MeOT2)) using the spin-coating method. When chloroform with the drop-casting method was used, similar performance as HFIP can be obtained but with poor film uniformity. This is probably due to the strong aggregation of the D-A polymers in the solution state (Figure S1).[35] We have noticed that many papers used drop-casting for device fabrication.[16,36] Hence, HFIP and the spin-coating were used for good film uniformity and reproducibility in this work. The figure of merit, μC^*, was extracted for

performance comparison among different materials. All the DPP polymers exhibited typical p-type OECT behaviors and worked in accumulation mode (Figure 2 and Figure S9). Among all the polymers, P(bgDPP-MeOT2) and P(lgDPP-MeOT2) with the strongest electron-donating moiety MeOT2, exhibited high g_m and high μC^* values (Table 1). P(bgDPP-MeOT2) exhibited the best OECT performance with a maximum transconductance of up to 5.33 mS with a film thickness of 64 nm, and high μC^* of up to 225 F cm^{-1} V^{-1} s^{-1}. P(bgDPP-MeOT2) showed negligible hysteresis during the forward and backward scans, suggesting its good and facile ion transport properties (Figure 2c&2d). With linear side chains, P(lgDPP-MeOT2) also exhibited outstanding OECT performance with high μC^* of 174±25 F cm^{-1} V^{-1} s^{-1} (Figure S9). In contrast, P(bgDPP-T2) and P(bgDPP-T) showed inferior OECT performance with μC^* values of 42±10 and 5.9±0.7 F cm^{-1} V^{-1} s^{-1}. Thus, the electron-donating properties play an important role in the OECT performance of the DPP polymers. Notably, polymer containing MeOT2 moiety showed lower threshold voltage (V_{Th}) than that containing T and T2 moieties. Interestingly, P(lgDPP-MeOT2) with linear side chains showed even lower V_{Th} (Figure S11). These results are consistent with the CV and spectroelectrochemistry studies. The criteria to judge whether a device works in OECT mode or electrolyte-gated organic field effect transistor (EGOFET) mode is the channel thickness dependence.[4,37] OECTs with different film thicknesses were also fabricated (Figure S10). Our devices showed clear film thickness dependent transconductance, suggesting that they indeed work in OECT mode. P(bgDPP-MeOT2) and P(lgDPP-MeOT2) show much higher μC^* values than other D-A copolymer OECT materials, e.g. 5.4 F cm^{-1} V^{-1} s^{-1} for PIBET-AO, 0.18 F cm^{-1} V^{-1} s^{-1} for P(gNDI-g2T) (Figure 3f, Figure S12 & Table S3).[26,27] The performance of the DPP polymers also outperforms most of the polythiophene systems that have been developed for many years.

Table 1 Summary of the OECTs Performance and Molecular Packing for the DPP Polymers.[a)]

Polymer	d [nm][a)]	$g_{m,max}$ [mS][a)]	$I_{on/off}$	V_{Th} [V][b)]	μ [cm^2 V^{-1} s^{-1}][c)]	C^* [F cm^{-3}]	μC^* [F cm^{-2} V^{-1} s^{-1}][d)]	τ_{on} [μs]	τ_{off} [μs]	$d_{lamellar}$ [Å]	$d_{\pi-\pi}$ [Å]
P(bgDPP-T)	29.1±0.8	0.019	2.2×10^3	−0.60	1.59±0.15	3.7±0.1	5.9±0.7	-	-	22.7	3.57
P(bgDPP-T2)	72.5±0.9	0.403	1.8×10^5	−0.57	0.50±0.11	84.1±1.5	42±10	-	-	20.7	3.51
P(lgDPP-MeOT2)	60.9±0.4	7.04	4.9×10^4	−0.17	2.15±0.27	80.8±1.4	174±25	578	63	18.6	3.45
P(bgDPP-MeOT2)	64.1±2.4	5.33	1.7×10^5	−0.33	1.63±0.14	120.0±2.4	195±21	516	30	20.7	3.55

All the OECT devices were operated in a 0.1 M NaCl aqueous solution. [a)] 14 devices with the same channel dimensions were tested and counted for each polymer (W/L =100/10 μm), V_{DS} = −0.6 V; [b)] The threshold voltage, V_{Th}, was determined by extrapolating the corresponding $I_{DS}^{1/2}$ *vs.* V_{GS} plots; [c)] Charge carrier mobility μ was calculated from the μC^* and the measured volumetric capacitance C^*; [d)] Materials' figure of merit μC^* were calculated from the measured transconductance.

Stressing measurements upon continuous biasing and long-term on-off switching tests were performed to demonstrate the stable operation of P(bgDPP-MeOT2) statically and dynamically. The drain current of the P(bgDPP-MeOT2) devices stayed almost unchanged atlow and moderate DC bias voltages, after continuous stressing for 10 minutes, while higher biasing condition only leads to a slight loss of ~1.7% on drain current (V_{DS}

= V_{GS} = −0.6 V) (Figure S13). Moreover, long-term on-off switching cycle tests of P(bgDPP-MeOT2) were also monitored (Figure 2e). The P(bgDPP-MeOT2) device exhibited good stability with current retention of 98.8% for 700 switching cycles and 89% for over 3000 cycles (Figure 2e & Figure S14), better than current state-of-the-art polythiophene based OECT channel materials.[15,17] Hence, P(bgDPP-MeOT2) also possesses outstanding stability upon continuous operation.

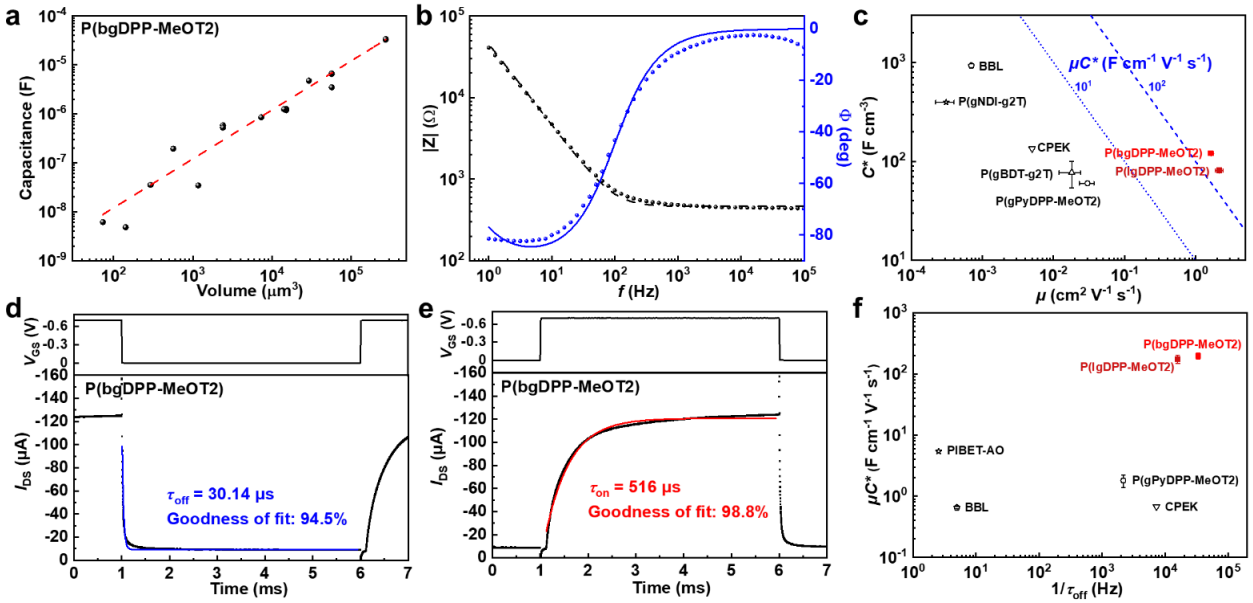

Figure 3 Capacitive, and transient behaviours of P(bgDPP-MeOT2). (a) Volume-capacitance relationship of P(bgDPP-MeOT2) was measured through the electrochemical impedance spectrum. The linear fit to the capacitance data was marked with the red dashed line. (b) The corresponding Bode and phase plot of P(bgDPP-MeOT2) with a channel area of 1 mm^2 and thickness of 56.8±4.2 nm. Data fits were performed via the equivalent circuit of $R_s(R_p||C)$. (c) Performance comparison via 2D μ-C^* plot for P(lgDPP-MeOT2), P(bgDPP-MeOT2), and other reported D-A polymer materials for OECTs. (d, e) Off- & on-time constant of P(bgDPP-MeOT2) obtained by applying a gate voltage pulse with a time scale of 5 ms. Blue and red lines were fitted through exponential decay function. W/L = 100/10 μm and d = 34.8±0.8 nm. (f) Performance comparison via 2D μC^*-$1/\tau_{off}$ plot for P(lgDPP-MeOT2), P(bgDPP-MeOT2), and other reported D-A polymer materials for OECTs.

To further understand the volumetric doping process of DPP polymers, the electrochemical impedance spectroscopy (EIS) technique was used. Gold electrodes coated with polymer films with certain areas and thicknesses were served as the working electrode with respect to Pt mesh as the counter electrode and Ag/AgCl pellet as the reference electrode. The effective capacitance could be extracted by fitting their EIS data via an equivalent circuit model ($R_s(R_p||C)$), *i.e.* a capacitor (C) connects a resistor (R_p) in parallel and further with a resistor (R_s) in series (Figure 3b). The extracted capacitances of P(bgDPP-MeOT2) upon different channel volumes were plotted, exhibiting a good linear relationship with the channel volume (Figure 3a). The volumetric capacitance (C^*) was extracted with a value of 120.0±2.4 F cm^{-3}. With linear EG chains, P(lgDPP-MeOT2) showed a volumetric capacitance of 80.8±1.4 F cm^{-3} (Figure S15 & Table 1), lower than that of P(bgDPP-

MeOT2). Based on the μC^* and C^* values, the hole mobility (μ) of both MeOT2 polymers can be calculated. P(bgDPP-MeOT2) showed hole mobility of 1.63±0.14 $cm^2\ V^{-1}\ s^{-1}$, and P(lgDPP-MeOT2) showed higher hole mobility of 2.15±0.27 $cm^2\ V^{-1}\ s^{-1}$ (Table 1). The mobility values are very close to their alkyl side chain counterparts measured in OFETs.[32,38] In OFETs, after introducing linear side chains, the mobility will also increase, largely due to less steric hindrance at the branching positions and a closer π-π stacking distance.[39,40]

To evaluate the response speed of P(bgDPP-MeOT2), time constants during turn-on and turn-off operation were both measured. As depicted in Figure 3d & 3e, after applying a 5 ms pulse voltage on the Ag/AgCl gate, temporal responses of drain current were recorded and fitted with the exponential decay function as described by the equation below,[41]

$$\boldsymbol{I_{DS}(t) = I_{DS,0} + a \times \exp(-t/\tau)} \quad (2)$$

where I_{DS}(t) represents the drain current at time t after applying the pulse gate bias, $I_{DS,0}$ represents the initial drain current before applying the pulse bias, a is a constant and τ is the time constant. The off-time constant (τ_{off}) and on-time constant (τ_{on}) were estimated to be 30 μs and 516 μs for P(bgDPP-MeOT2, with a channel geometry of 100 μm /10 μm (W/L). Obviously, both off- and on-time constants of P(bgDPP-MeOT2) reach the top-performing level among reported polymers, including D-A polymers and polythiophenes (Figure 3f & Table S3). According to literature, the time constant of p-type OECT is mainly dominated by the ion injection process and the removal of holes from the source electrode. Gaining higher hole mobility or volumetric capacitance can effectively enhance the response speed. In specific, P(lgDPP-MeOT2) also exhibited fast response characteristic on the transient behaviors. On- & off-time constant of P(lgDPP-MeOT2) under similar channel geometry achieved 578 μs and 63 μs, respectively (Figure S16). To fully compare thecomprehensive performance of P(bgDPP-MeOT2) with other reported polymers, the reciprocal of on- and off-time constant and the μC^* are plotted in Figure 3f.[15,16,26,34,42,43]

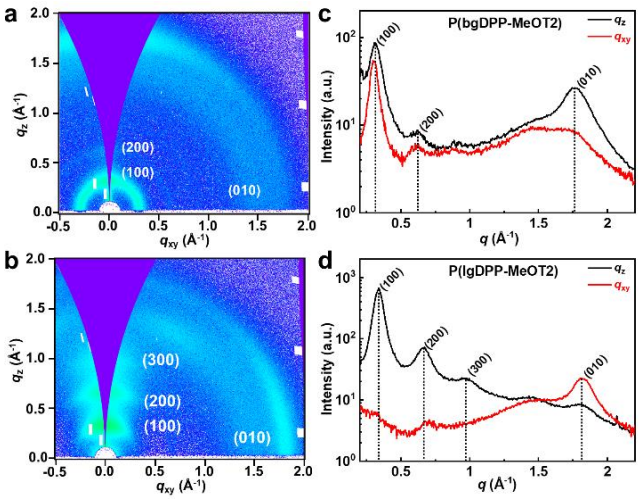

Figure 4 2D-GIWAXS patterns of (a) P(bgDPP-MeOT2) and (b) P(lgDPP-MeOT2); (c-d) The corresponding line cuts of P(bgDPP-MeOT2) and P(lgDPP-MeOT2). Cuts along the q_{xy} direction (red) represent scattering in the plane of the substrate, while the scattering in the q_z direction (black) results from out-of-plane scattering.

Crystallinity and molecular packing of conjugated polymers strongly influence water uptake, ion transport, and charge carrier transport in the polymer bulk. Two-dimensional (2D) GIWAXS was employed to reveal the differences among the polymers. All bgDPP polymers oriented preferably in a face-on fashion, while P(lgDPP-MeOT2) with linear EG chains, oriented predominantly with edge-on (Figure 4). P(lgDPP-MeOT2) exhibited a closer π-π stacking distance of 3.45 Å, smaller than those of the bgDPP polymers (3.51-3.57 Å), consisting with our previous absorption spectra analysis and mobility results (Figure S17). In addition, P(lgDPP-MeOT2) also exhibited three orders of lamellar scattering peaks, (100), (200), and (300), indicating the well-packed polymer side chains compared with those with branched side chains. For conjugated polymers with highly ordered crystallites, the injection of hydrated ions into polymer bulk may induce destruction of morphology and then impede charge transport between adjacent crystallites.[13,44] Therefore, less ordered packing of P(bgDPP-MeOT2) might contribute to the enhanced penetration of hydrated ions into the polymer bulk (higher C^*) and faster temporal response, though its hole mobility is slightly sacrificed.

Conclusions

In conclusion, we have systematically explored the influences of the donor, side chain, molecular weight, and processing conditions to solve the low-performance issue in D-A conjugated polymers. The high-performance of P(bgDPP-MeOT2) can be attributed to the following molecular design and device fabrication considerations: (i) strong electron-donating moiety MeOT2 reduces the ionization potential of DPP polymers, leading to a low threshold voltage and high volumetric capacitance; (ii) the branched EG chains guarantee enough solubility for high molecular weight polymers and also facilitate ion injection/ejection in the polymer bulk; (iii) optimized polymerization method allows comparable molecular weight and hole mobility as its alkyl side chain counterpart; (iv) the "uncommon" polar solvent HFIP is used to disaggregate the polymers for better film quality. These efforts lead to a high μC^* (> 200 F cm^{-1} V^{-1} s^{-1}), high hole mobility (>2 cm^2 V^{-1} s^{-1}), and fast response (τ_{off} 30 μs; τ_{on} 516 μs), much higher than other D-A polymer-based OECT materials (Table S3). Considering that most n-type conjugated polymers are based on D-A copolymers, we believe that our study will not only benefit high-performance and fast-response p-type OECT materials but also will be valuable for n-type OECT materials whose performance lags far behind that of the p-type ones.

Conflicts of interest

There are no conflicts to declare.

Acknowledgements

This work is supported by the Guangdong Science and Technology Project (2019B010934001) and the Beijing Natural Science Foundation (2192020). The computational part is supported by High-performance Computing Platform of Peking University. The scattering component in this manuscript is supported by U.S. Department of Energy, Office of Science, Office of Basic Energy Science under award number of DE-SC0019361.

Hanyu Jia, Zhen Huang, and Peiyun Li contributed equally to this work.

References

[1] J. Rivnay, R. M. Owens, G. G. Malliaras, *Chem. Mater.*, **2013**, *26*, 679.

[2] B. D. Paulsen, K. Tybrandt, E. Stavrinidou, J. Rivnay, *Nat. Mater.*, **2020**, *19*, 13.

[3] G. D. Spyropoulos, J. N. Gelinas, D. Khodagholy, *Sci. Adv.*, **2019**, *5*, eaau7378.

[4] J. Rivnay, P. Leleux, M. Ferro, M. Sessolo, A. Williamson, D. A. Koutsouras, D. Khodagholy, M. Ramuz, X. Strakosas, R. M. Owens, C. Benar, J. M. Badier, C. Bernard, G. G. Malliaras, *Sci. Adv.*, **2015**, *1*, e1400251.

[5] V. Venkatraman, J. T. Friedlein, A. Giovannitti, I. P. Maria, I. McCulloch, R. R. McLeod, J. Rivnay, *Adv. Mater.*, **2018**, *5*, 1800453.

[6] O. Parlak, S. T. Keene, A. Marais, V. F. Curto, A. Salleo, *Sci. Adv.*, **2018**, *4*, eaar2904.

[7] A. M. Pappa, D. Ohayon, A. Giovannitti, I. P. Maria, A. Savva, I. Uguz, J. Rivnay, I. McCulloch, R. M. Owens, S. Inal, *Sci. Adv.*, **2018**, *4*, eaat0911.

[8] P. Li, T. Lei, L. Ding, *Sci. Bull.*, **2020**, *65*, 1141.

[9] Y. van de Burgt, E. Lubberman, E. J. Fuller, S. T. Keene, G. C. Faria, S. Agarwal, M. J. Marinella, A. Alec Talin, A. Salleo, *Nat. Mater.*, **2017**, *16*, 414.

[10] Y. van de Burgt, A. Melianas, S. T. Keene, G. Malliaras, A. Salleo, *Nat. Electron.*, **2018**, *1*, 386.

[11] D. Khodagholy, T. Doublet, P. Quilichini, M. Gurfinkel, P. Leleux, A. Ghestem, E. Ismailova, T. Herve, S. Sanaur, C. Bernard, G. G. Malliaras, *Nat. Commun.*, **2013**, *4*, 1575.

[12] P. Gkoupidenis, N. Schaefer, B. Garlan, G. G. Malliaras, *Adv. Mater.*, **2015**, *27*, 7176.

[13] R. Giridharagopal, L. Q. Flagg, J. S. Harrison, M. E. Ziffer, J. Onorato, C. K. Luscombe, D. S. Ginger, *Nat. Mater.*, **2017**, *16*, 737.

[14] C. Cea, G. D. Spyropoulos, P. Jastrzebska-Perfect, J. J. Ferrero, J. N. Gelinas, D. Khodagholy, *Nat. Mater.*, **2020**, *19*, 679.

[15] A. Giovannitti, D. T. Sbircea, S. Inal, C. B. Nielsen, E. Bandiello, D. A. Hanifi, M. Sessolo, G. G. Malliaras, I. McCulloch, J. Rivnay, *Proc. Natl. Acad. Sci. U. S. A.*, **2016**, *113*, 12017.

[16] C. B. Nielsen, A. Giovannitti, D. T. Sbircea, E. Bandiello, M. R. Niazi, D. A. Hanifi, M. Sessolo, A. Amassian, G. G. Malliaras, J. Rivnay, I. McCulloch, *J. Am. Chem. Soc.*, **2016**, *138*, 10252.

[17] M. Moser, T. C. Hidalgo, J. Surgailis, J. Gladisch, S. Ghosh, R. Sheelamanthula, Q. Thiburce, A. Giovannitti, A. Salleo, N. Gasparini, A. Wadsworth, I. Zozoulenko, M. Berggren, E. Stavrinidou, S. Inal, I. McCulloch, *Adv. Mater.*, **2020**, *32*, e2002748.

[18] S. Inal, G. G. Malliaras, J. Rivnay, *Nat. Commun.*, **2017**, *8*, 1767.

[19] S. M. Kim, C. H. Kim, Y. Kim, N. Kim, W. J. Lee, E. H. Lee, D. Kim, S. Park, K. Lee, J. Rivnay, M. H. Yoon, *Nat. Commun.*, **2018**, *9*, 3858.

[20] H. Sun, M. Vagin, S. Wang, X. Crispin, R. Forchheimer, M. Berggren, S. Fabiano, *Adv. Mater.*, **2018**, *30*, 1704916.

[21] M. Kawan, T. C. Hidalgo, W. Du, A.-M. Pappa, R. M. Owens, I. McCulloch, S. Inal, *Mater. Horiz.*, **2020**, *7*, 2348.

[22] J. Yang, Z. Y. Zhao, S. Wang, Y. L. Guo, Y. Q. Liu, *Chem*, **2018**, *4*, 2748.

[23] H. Jia, T. Lei, *J. Mater. Chem. C*, **2019**, *7*, 12809.

[24] X. Yan, M. Xiong, J. T. Li, S. Zhang, Z. Ahmad, Y. Lu, Z. Y. Wang, Z. F. Yao, J. Y. Wang, X. Gu, T. Lei, *J. Am. Chem. Soc.*, **2019**, *141*, 20215.

[25] S. Fratini, M. Nikolka, A. Salleo, G. Schweicher, H. Sirringhaus, *Nat. Mater.*, **2020**, *19*, 491.

[26] Y. Wang, E. Zeglio, H. Liao, J. Xu, F. Liu, Z. Li, I. P. Maria, D. Mawad, A. Herland, I. McCulloch, W. Yue, *Chem. Mater.*, **2019**, *31*, 9797.

[27] A. Giovannitti, C. B. Nielsen, D. T. Sbircea, S. Inal, M. Donahue, M. R. Niazi, D. A. Hanifi, A. Amassian, G. G. Malliaras, J. Rivnay, I. McCulloch, *Nat. Commun.*, **2016**, *7*, 13066.

[28] A. Giovannitti, I. P. Maria, D. Hanifi, M. J. Donahue, D. Bryant, K. J. Barth, B. E. Makdah, A. Savva, D. Moia, M. Zetek, P. R. F. Barnes, O. G. Reid, S. Inal, G. Rumbles, G. G. Malliaras, J. Nelson, J. Rivnay, I. McCulloch, *Chem. Mater.*, **2018**, *30*, 2945.

[29] A. Giovannitti, R. B. Rashid, Q. Thiburce, B. D. Paulsen, C. Cendra, K. Thorley, D. Moia, J. T. Mefford, D. Hanifi, D. Weiyuan, M. Moser, A. Salleo, J. Nelson, I. McCulloch, J. Rivnay, *Adv. Mater.*, **2020**, *32*, e1908047.

[30] Z. Yi, S. Wang, Y. Liu, *Adv. Mater.*, **2015**, *27*, 3589.

[31] B. Carsten, F. He, H. J. Son, T. Xu, L. Yu, *Chem. Rev.*, **2011**, *111*, 1493.

[32] R. Di Pietro, T. Erdmann, J. H. Carpenter, N. Wang, R. R. Shivhare, P. Formanek, C. Heintze, B. Voit, D. Neher, H. Ade, A. Kiriy, *Chem. Mater.*, **2017**, *29*, 10220.

[33] P. Schmode, D. Ohayon, P. M. Reichstein, A. Savva, S. Inal, M. Thelakkat, *Chem. Mater.*, **2019**, *31*, 5286.

[34] D. Khodagholy, J. Rivnay, M. Sessolo, M. Gurfinkel, P. Leleux, L. H. Jimison, E. Stavrinidou, T. Herve, S. Sanaur, R. M. Owens, G. G. Malliaras, *Nat. Commun.*, **2013**, *4*, 2133.

[35] M. Li, H. Bin, X. Jiao, M. M. Wienk, H. Yan, R. A. J. Janssen, *Angew. Chem., Int. Ed.*, **2020**, *59*, 846.

[36] A. Giovannitti, K. J. Thorley, C. B. Nielsen, J. Li, M. J. Donahue, G. G. Malliaras, J. Rivnay, I. McCulloch, *Adv. Funct. Mater.*, **2018**, *28*, 1706325.

[37] E. Zeglio, O. Inganas, *Adv. Mater.*, **2018**, *30*, e1800941.

[38] Y. Li, P. Sonar, S. P. Singh, M. S. Soh, M. van Meurs, J. Tan, *J. Am. Chem. Soc.*, **2011**, *133*, 2198.

[39] T. Lei, J. H. Dou, J. Pei, *Adv. Mater.*, **2012**, *24*, 6457.

[40] Z. Wang, Z. Liu, L. Ning, M. Xiao, Y. Yi, Z. Cai, A. Sadhanala, G. Zhang, W. Chen, H. Sirringhaus, D. Zhang, *Chem. Mater.*, **2018**, *30*, 3090.

[41] D. A. Bernards, G. G. Malliaras, *Adv. Funct. Mater.*, **2007**, *17*, 3538.

[42] A. Savva, R. Hallani, C. Cendra, J. Surgailis, T. C. Hidalgo, S. Wustoni, R. Sheelamanthula, X. Chen, M. Kirkus, A. Giovannitti, A. Salleo, I. McCulloch, S. Inal, *Adv. Funct. Mater.*, **2020**, *30*, 1907657.

[43] S. Inal, J. Rivnay, P. Leleux, M. Ferro, M. Ramuz, J. C. Brendel, M. M. Schmidt, M. Thelakkat, G. G. Malliaras, *Adv. Mater.*, **2014**, *26*, 7450.

[44] L. Q. Flagg, C. G. Bischak, J. W. Onorato, R. B. Rashid, C. K. Luscombe, D. S. Ginger, *J. Am. Chem. Soc.*, **2019**, *141*, 4345.